A Temperature Phantom to Probe the Ensemble Average Propagator Asymmetry: an In-Silico Study

Marco Pizzolato, Demian Wassermann, Tanguy Duval, Jennifer S. W. Campbell, Timothé Boutelier, Julien Cohen-Adad, Rachid Deriche

A Temperature Phantom to Probe the Ensemble Average Propagator Asymmetry: an In-Silico Study

Marco Pizzolato[1]*, Demian Wassermann[1], Tanguy Duval[2], Jennifer S.W. Campbell[3], Timothé Boutelier[4], Julien Cohen-Adad[2], and Rachid Deriche[1]

[1] Athena, Inria Sophia Antipolis - Méditerranée, France
[2] Polytechnique Montreal, Montreal, Quebec, Canada
[3] McGill University, Montreal, Quebec, Canada
[4] Olea Medical, La Ciotat, France

Abstract. The detection and quantification of asymmetry in the Ensemble Average Propagator (EAP) obtained from the Diffusion-Weighted (DW) signal has been shown only for theoretical models. EAP asymmetry appears for instance when diffusion occurs within fibers with particular geometries. However the quantification of EAP asymmetry corresponding to such geometries in controlled experimental conditions is limited by the difficulty of designing fiber geometries on a micrometer scale. To overcome this limitation we propose to adopt an alternative paradigm to induce asymmetry in the EAP. We apply a temperature gradient to a spinal cord tract to induce a corresponding diffusivity profile that alters locally the diffusion process to be asymmetric. We simulate the EAP and the corresponding complex DW signal in such a scenario. We quantify EAP asymmetry and investigate its relationship with the applied experimental conditions and with the acquisition parameters of a Pulsed Gradient Spin-Echo sequence. Results show that EAP asymmetry is sensible to the applied temperature-induced diffusivity gradient and that its quantification is influenced by the selected acquisition parameters.

Keywords: Diffusion MRI, phantom, EAP, asymmetry, temperature, viscosity

1 Introduction

The Ensemble Average Propagator (EAP) obtained from the Diffusion-Weighted (DW) signal in Magnetic Resonance Imaging (MRI) expresses the displacement probability of spin-bearing particles [2]. Although the displacement probability is commonly considered axially symmetric along a diffusion direction, this is generally not the case in tissue. The displacement probability, hence the EAP, may show asymmetry due to the characteristics of tissue geometry, as recently reported [7, 8]. For instance, a relationship between EAP asymmetry and axonal tortuosity variation rates - corresponding to different levels of axonal compression - is described in [8]. However the task of measuring asymmetry on real data is non-trivial, therefore here we present an in-silico study to

*The author expresses his thanks to Olea Medical and to the Provence-Alpes-Côte d'Azur Regional Council for providing grant and support.

assess the feasibility of a physical phantom to measure EAP asymmetry via DW-MRI, highlighting the relationship between the controllable experimental parameters and said asymmetry.

Technical difficulties in building a physical phantom for DW-MRI mainly consist on designing axonal geometries at micrometer scale with controllable properties and tissue-like diffusion characteristics. For instance, at the present moment building a phantom resembling compressed axons with different degrees of compression is very challenging. An alternative solution to induce diffusion asymmetry needs to be found. Other difficulties are related to the measurement of the asymmetry with the DW signal. Particularly, EAP asymmetry may only be retrieved from the complex DW signal thus implying that a problem of observabilty of the phenomenon also arises, specially with reference to the high sensibility of the signal's phase to noise and bulk movement. In this work, however, we mainly discuss the physical principles underlying the proposed phantom and investigate the relationships with the controllable parameters of a Pulsed Gradient Spin Echo (PGSE) sequence.

In the study we predict the DW signal acquired in a possible real experimental setup designed with the precise scope of inducing diffusion asymmetry in the sampled tissue. The adopted strategy consists in applying a temperature gradient in a spinal cord tract, along the direction of the fibers, to obtain a spatially localized diffusion coefficient. We refer to this as a temperature-induced diffusivity gradient. The diffusion coefficient will be forced to vary monotonically with the position coordinate, i.e. it will increase as the spatial location gets closer to the highest temperature position. In this way, at each point along the fiber, a water particle moving towards the highest temperature position will experience higher diffusivity values than a particle moving in the opposite direction, thus leading to asymmetry in the EAP.

This work investigates the relationship between the temperature-induced diffusivity gradient and EAP asymmetry in order to assess the feasibility in principle of a real DW signal acquisition with a PGSE sequence. To do so we first describe the proposed phantom and the related assumptions. Then we consider an applied temperature gradient and derive the corresponding spatial diffusivity profile induced in the phantom. With this setup we simulate a PGSE acquisition of the phantom with voxels located along its longitudinal direction, that is the direction aligned with the fibers. For each voxel we recover the complex DW signal and then compute the EAP from this to quantify the asymmetry. We then present results as the experimental conditions and acquisition parameters variate, highlighting the dependency of EAP asymmetry on the temperature-induced diffusivity gradient. Finally we discuss the feasibility of the proposed technique and its inherent limitations.

2 Phantom Design and Experimental Setup

The simulation considers a temperature gradient applied to a longitudinal spinal cord tract of length l, where the longitudinal direction corresponds to that parallel to the fibers. The temperature gradient is generated in the spinal cord by heating up the two extremities at two different temperatures maintained constant during time: one extremity at low temperature T_L and the other at high temperature T_H. The schematic represen-

tation of the experimental setup is illustrated in fig. 1. The corresponding temperature

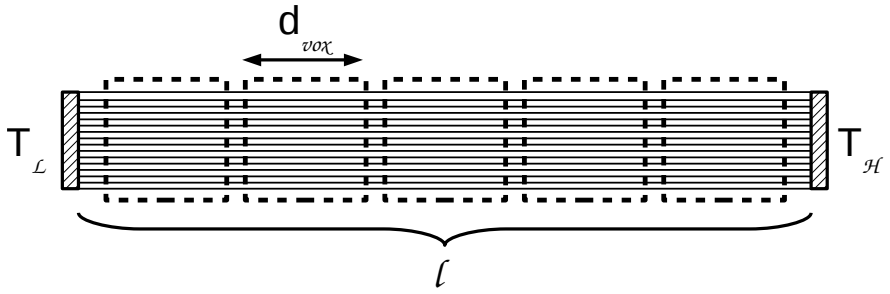

Fig. 1. Schematic representation of the proposed experimental setup. A spinal cord tract of length l lies between two gears maintained at two different constant temperatures, T_L and T_H, the fibers composing the spinal cord tract being aligned along the direction connecting said gears namely the longitudinal direction. Acquisition voxels with side d_{vox} are located along the longitudinal direction so that to collect signal from tissue at different mean temperatures.

profile along the spinal cord tract is consequently obtained, as discussed in section 3.

The temperature difference between the extremities produces a profile $T(z)$ of varying temperature along the longitudinal direction z. The spatially-localized temperature $T(z)$ in the spinal cord tract is used to obtain the corresponding diffusivity value $D(T)$. The diffusivity values are computed along the spinal cord in order to obtain a diffusivity profile. Furthermore, values are conveniently scaled to simulate Cerebrospinal Fluid ($D_{csf}(T)$), Grey Matter ($D_{gm}(T)$) and White Matter ($D_{wm}(T)$) diffusivities.

The DW-MRI acquisition is simulated bi-dimensionally, similarly to [8]. The spinal cord tract is discretized in adjacent spatial units corresponding to voxels distributed along the longitudinal direction (fig. 1). The tissue underlying each voxel is considered as being composed of straight fibers with infinitesimal thickness. Water particles diffusing within these fibers are subjected to the locally observed temperature-induced diffusivity gradient. Therefore the simulated signal takes into account the local values of the diffusion coefficient. Voxels size $d_{vox}(m)$ and PGSE parameters such as maximum diffusion gradient strength $G_{max}(T/m)$, pulse duration $\delta(s)$ and separation between pulses $\Delta(s)$ are taken into account. Finally EAP asymmetry is calculated for each voxel and studied as function of the applied temperature gradient.

The following section provides details about the assumed temperature gradient along the longitudinal direction of the spinal cord tract.

3 Applied Temperature Gradient

In this section we present the assumptions made for the temperature profile applied along the spinal cord tract.

The spinal cord tract is considered as a homogeneous rod extending longitudinally to the fibers' direction. Due to the long time required for the MR acquisition, stationary

conditions are assumed. Therefore no transient dynamic is considered for the calculation of the resulting temperature gradient which will then be constant. Hence, the temperature gradient along the rod is obtained as the steady-state solution of the heat equation when the two extremities are maintained at two different constant temperatures, rendering a linear temperature profile

$$T(z) = z \cdot \frac{T_H - T_L}{l} + T_L \tag{1}$$

where T_L is the temperature in $z = 0$, T_H is the temperature applied in $z = l$ and l is as usual the length of the spinal cord tract, fig. 1. Temperature will be henceforth expressed in Celsius degrees ($^\circ C$).

The following section reports how we calculate the diffusivity profile along the spinal cord tract, for different tissue types, given the temperature profile.

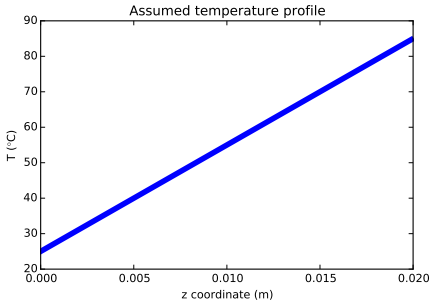

Fig. 2. Temperature as function of the position as found from the steady-state solution of the heat equation. Maximum distance $l = 0.02\,m$, $T_L = 25^\circ C$, $T_H = 85^\circ C$.

4 Induced Diffusivity Profile

In this section we calculate the diffusivity profile for different tissues as resulting from the application of a temperature gradient having the characteristics reported in section 3. The diffusivity profile along the longitudinal direction of the spinal cord tract depends on the assumed temperature profile. However the diffusion coefficient depends also on the characteristics of the liquid in which particles diffuse and on the geometrical properties of the particles themselves. These dependencies are well described by the Stokes-Einstein equation:

$$D(T) = \frac{k_B(T + 273.15)}{6\pi r\eta} \tag{2}$$

where k_B is the Boltzmann constant, r the radius of the spherical particle and η the dynamic viscosity. Assuming free diffusion of water particles, the radius can be approximated by applying the inverse formula of eq. (2) while knowing the reference values at

$T = 25°C$ of dynamic viscosity $\eta_{fw}^{25}\,(Kg/ms)$ and diffusivity $D_{fw}^{25} = 2.299 \cdot 10^{-9}\,m^2/s$ [4]. However, dynamic viscosity is function of temperature and cannot simply be a constant. Therefore to calculate η_{fw}^{25} we employ the equation describing the relationship between free water viscosity and temperature [1], which is accurate to within 2.5% from $0°C$ to $370°C$:

$$\eta_{fw}(T) = 2.414 \cdot 10^{-5} \cdot 10^{\frac{247.8}{T+273.15-140.0}}. \tag{3}$$

Using eq. (3) the predicted free water viscosity at $25°C$ is $\eta_{fw}^{25} = 0.891 \cdot 10^{-3} Kg/ms$, then we approximate the radius inverting eq. (2) obtaining $r \approx 1.066^{-10}\,m$.

Water diffusivity in tissues is lower than that of free water for a same temperature. Indeed dynamic viscosity increases in tissue accordingly to its microstructural properties. Assuming a constant temperature of $37.9°C$ in the living brain tissue [5], the dynamic viscosity in CSF ($\eta_{csf}^{37.9}$), GM ($\eta_{gm}^{37.9}$) and WM ($\eta_{wm}^{37.9}$) can be calculated from eq. (2) knowing the corresponding diffusivity values, which can be found to be [3] $D_{csf}^{37.9} = 2.9 \cdot 10^{-9}\,m^2/s$, $D_{gm}^{37.9} = 0.89 \cdot 10^{-9}\,m^2/s$ and $D_{wm}^{37.9} = 0.73 \cdot 10^{-9}\,m^2/s$.

Having the viscosity values for the different tissues at $37.9°C$, we calculate an empirical scaling factor between free water viscosity as function of temperature in eq. (3), and tissue viscosity. Therefore viscosity values could be found as corresponding to $\eta_{csf} \approx 1.09 \cdot \eta_{fw}$, $\eta_{gm} \approx 3.54 \cdot \eta_{fw}$ and $\eta_{wm} \approx 4.32 \cdot \eta_{fw}$. We note that the scaling factor for gray matter is in agreement with the assumed value in [6]. These factors are adopted to scale eq. (3) to calculate the dynamic viscosity at all the temperatures for the different tissue types. By substituting η in eq. (2) with the opportunely scaled version of eq. (3), we compute the diffusivity profiles along the spinal cord tract, as shown in fig. 3. We point out that diffusion coefficients used to obtain the scaling factors are the

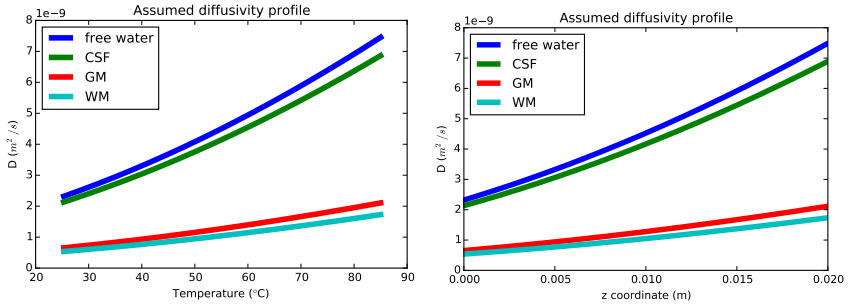

Fig. 3. Diffusion coefficient profile for different tissue types as function of the temperature (left) and of the position in the spinal cord tract (right).

apparent diffusion coefficients for the corresponding tissues. Particularly the apparent diffusion coefficient in a tissue can be seen as the product $\lambda \cdot D^*$ where D^* is the diffusion coefficient of the media, which depends on temperature and viscosity, and λ is the tortuosity coefficient which solely depends on geometry. For instance in WM the tortuosity changes with the considered diffusion direction, i.e. the diffusion coefficient

along the direction parallel to fibers is higher than $D_{wm}^{37.9}$. However we use this value aware that it renders a lower bound for the diffusivity profile along fibers. Moreover the diffusivity profile of CSF and GM may only be considered within the fibers for the sake of representing 1D diffusion in the corresponding tissues.

In the next section we calculate the Ensemble Average Propagator for adjacent voxels located along the longitudinal direction of the spinal cord tract, and obtain the corresponding complex DW signal. We then describe the quantification of the asymmetry of the EAP obtained from the signal.

5 EAP with Temperature-induced Diffusivity Gradient

In this section we present the derivation of the Ensemble Average Propagator (EAP) when a temperature-induced diffusivity gradient is applied to the spinal cord tract. The obtained EAP is used to recover the complex DW signal via a Fourier relationship [9]. From the complex signal the original EAP can be recovered exploiting the inverse relationship and its asymmetry can be quantified as presented below.

The EAP is obtained in 2D, similarly to [8], by considering diffusion within straight fibers with infinitesimal thickness. Fibers are considered to be aligned along the longitudinal direction of the spinal cord tract. Assuming that particles diffuse freely along the fiber, their displacement follows a normal distribution with variance $2D(T,\eta)t_d$, where t_d is the diffusion time and $D(T,\eta)$ is the diffusion coefficient as function of temperature and dynamic viscosity. Then, the probability of a particle experiencing a net displacement along the z-axis Δz can be approximated by

$$P(\Delta z, t_d, T, \eta) = \frac{1}{\sqrt{4\pi D(T,\eta)t_d}} e^{-\frac{\Delta z^2}{4D(T,\eta)t_d}} \tag{4}$$

which depends on the temperature and, consequently, on the location of the particle within the spinal cord tract. We note that since both the temperature and the dynamic viscosity are function of the particle location z, eq. (4) can be rewritten as

$$P(\Delta z|z, t_d) = \frac{1}{\sqrt{4\pi D(z+\Delta z)t_d}} e^{-\frac{\Delta z^2}{4D(z+\Delta z)t_d}} \tag{5}$$

where we highlight the dependency of the diffusivity on the location. The fact that the diffusion coefficient is not constant but varies monotonically with the location is the cause of the asymmetry of eq. (5), which will be reflected in the EAP.

The EAP that will be considered for calculating the signal is that accounting for the ensemble of particles within the whole voxel. To do so we discretize the length of the spinal cord tract l in locations z_i each $1\mu m$. At each location z_i we evaluate eq. (5) over an observation frame large enough to observe the Gaussian decay, thus obtaining a local propagator. Particularly the local propagator is calculated from a maximum negative displacement $-\Delta z_{max}$ to a maximum positive displacement Δz_{max} with $\Delta z_{max} = (6D_{fw}^{37.9} t_d)^{\frac{1}{2}}$. The final EAP for each voxel is obtained by numerical integration of the local propagators calculated for the locations z_i within the voxel's limits,

considering voxels of size d_{vox} ($= 1\,mm$ in the rest), corresponding to the numerical implementation of

$$EAP(\Delta z; t_d) = \int_{z \in voxel} \rho_0 P(\Delta z | z, t_d)\, dz \tag{6}$$

where ρ_0 is the constant initial density of particles.

The resolution of the calculated EAP, i.e. the minimum observable displacement r, is calculated from the maximum gradient strength as $r = 1/G_{max}$. Sequence parameters such as δ and Δ are chosen in agreement with plausible real values to account for the chosen t_d. The voxel-averaged EAP is used to calculate the complex signal via Fourier transform under narrow pulse approximation [8, 9].

The final goal is to quantify the asymmetry of the EAP calculated for each voxel. To do this the EAP is re-computed from the complex signal and the EAP asymmetry is then calculated as the Hellinger distance between each EAP and its axially reflected version [8]

$$H^2 = \frac{1}{2} \int \left(\sqrt{EAP(\mathbf{r}|t_d)} - \sqrt{EAP(-\mathbf{r}|t_d)} \right)^2 d\mathbf{r} \tag{7}$$

where $\mathbf{r} = (0, \Delta z)$ and where $0 \leq H \leq 1$, 0 corresponding to equality, i.e. perfect symmetry, and 1 to maximum inequality, i.e. perfect asymmetry.

6 Results

Results show that the amount of EAP asymmetry increases as the temperature gradient increases. Particularly, acquisitions with increasing T_H (i.e. $45, 55, 65, 75, 85\,^\circ C$) while keeping T_L fixed (i.e. $25\,^\circ C$) will lead to an increasing EAP asymmetry. This relation can be predicted with the developed model such as in fig. 6 left. In the following more detailed results and related comments are provided.

EAP changes slowly across voxels. Under a determined temperature gradient it is hard to visually distinguish between the EAP for different voxels acquired along the spinal cord tract. For instance, fig. 4 shows the EAP for different voxels at different locations. However values of the EAP change accordingly to the underlying mean diffusivity rates which change based on the voxel location. Indeed fig. 5 left shows the norm of the differences between the EAP of each voxel with respect to that of the coldest voxel, as the location gets closer to the highest temperature position $z = l$. A linear relationship can be found.

EAP asymmetry for different voxels remains constant. The plot in fig. 5 right shows the EAP asymmetry for voxels at locations closer and closer to the highest temperature position $z = l$. Contrary to fig. 5 left, here there are no differences between voxels. Indeed the amount of EAP asymmetry, since the diffusivity profile is quasi-linear, is constant. The only actual differences between voxels have to be ascribed to the slight non-linearity of the temperature-induced diffusivity gradient (fig. 3).

EAP asymmetry increases with the temperature-induced diffusivity gradient. The most interesting result is that, despite EAP asymmetry across voxels remains substantially constant, the amount of asymmetry increases with the temperature gradient (for a given dynamic viscosity or tissue type). For instance fig. 5 right shows EAP asymmetries for different temperature gradients, $25-45\,^\circ C$, $25-65\,^\circ C$ and $25-85\,^\circ C$.

The quasi-linear relationship between EAP asymmetry and temperature gradient can be better appreciated in fig. 6 left.

EAP asymmetry increases with the diffusion time. When particles can diffuse for a longer time they can probe a wider range of diffusivity values. Therefore the differences between the EAP values calculated for positive and negative displacements are greater. However the asymmetry dependency on the diffusion time seems to follow a saturative profile (fig. 6 right).

Maximum gradient strength seems to have little influence on EAP asymmetry. As opposed to what stated in [8], when fibers are straight the maximum gradient strength G_{max}, i.e. the spatial resolution of the EAP, seems not to influence the asymmetry. In this experiment it was found that increasing the resolution simply leads to convergence of the asymmetry value.

The selected dynamic viscosity influences the results. Depending on the considered type of tissue (dynamic viscosity) the results can be more or less relevant. Indeed for a given temperature gradient, considering the dynamic viscosity of free water diffusion leads to a greater diffusivity gradient than that obtained considering white matter tissue (fig. 3 left). The considered tissue type affects the resulting EAP as illustrated in fig. 7.

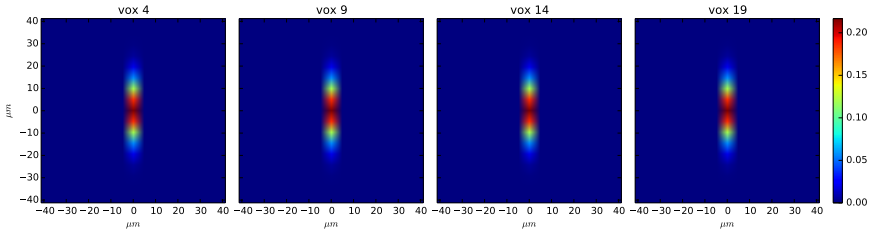

Fig. 4. EAPs for voxels at different location. As the voxel number increases the location is closer to the hottest point ($t_d = 90ms$, $G_{max} = 500mT/m$). Results obtained for WM ($25-45°C$).

7 Discussion

The objective of this work is to propose a method for quantifying the asymmetry of the Ensemble Average Propagator with a real physical phantom, and assess its feasibility. Designing a physical phantom for measuring asymmetry is important in order to validate the use of EAP asymmetry as tissue biomarker as in the case of compressed axons [8]. However it imposes several challenges. Conceptual designs accounting for specific fiber geometries inducing asymmetry face the limit of the scale required to appreciate constrained diffusion. To overcome this practical issue we propose to induce diffusion asymmetry in tissue by applying a temperature gradient to, in this case, a spinal cord tract. The temperature gradient results in a corresponding diffusivity profile which alters

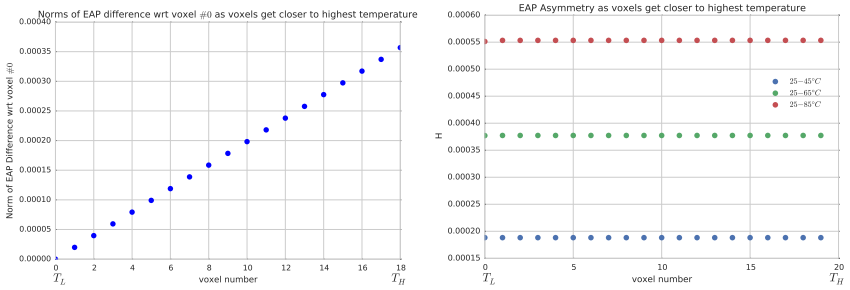

Fig. 5. Left: norm of difference between the EAP of a voxel with respect to the EAP measured for the voxel #0 corresponding to that showing the lowest temperature in the range $25-85°C$. Right: Hellinger distance for different voxels and temperature gradients. Results obtained for WM ($t_d = 90\,ms$, $G_{max} = 1\,T/m$).

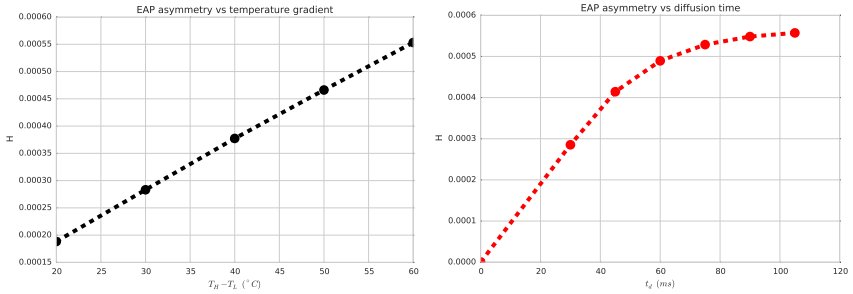

Fig. 6. EAP asymmetry averages (among the voxels) as function of: temperature gradient with $T_L = 25°C$ and $t_d = 90\,ms$ (left); diffusion time with $25-85°C$ (right). Results obtained for WM ($G_{max} = 1\,T/m$).

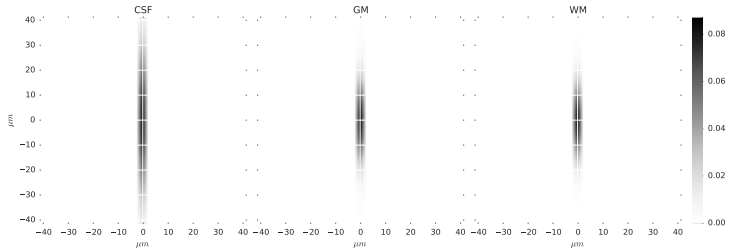

Fig. 7. EAP for straight fibers assuming diffusion as in Cerebrospinal Fluid, Grey Matter and White Matter ($t_d = 90\,ms$, $G_{max} = 1\,T/m$).

the local diffusion process to be asymmetric since the displacement of particles diffusing towards locations with higher diffusion coefficients is in principle greater than that towards locations with lower diffusivity.

In this work we present the study of how experimental conditions and acquisition parameters influence the generation and the quantification (via DW signal) of EAP asymmetry respectively. A first consideration is that the proposed method shows low sensitivity of EAP asymmetry to the diffusivity profile induced by the tested temperature gradients. Indeed, as opposed to the results reported for asymmetry induced by the fiber geometry in [8], here values of asymmetry are low. This might lead to issues in detecting different levels of asymmetry in the physical phantom. However results show that the amount of EAP asymmetry increases almost linearly with the temperature gradient and that asymmetry can be better quantified with a longer diffusion time t_d in the PGSE sequence. These observations suggest that an experiment investigating the relationship between EAP asymmetry and the temperature-induced diffusivity gradient is feasible. More precisely, a possible experimental strategy is to perform acquisitions of the spinal cord tract at different temperature-induced diffusivity gradients to replicate results such as those in fig. 5 right and fig. 6 left.

Further investigations and simulations are required. A next step is to release the infinitesimal thickness assumption that constrains particle trajectories to lie on a line. If particles were free to move along different directions their global displacement would affect differently the EAP and its asymmetry. Moreover, additive signal noise should be taken into account. Particular attention should be payed to the choice of diffusion time t_d and maximum gradient strength G_{max}. Indeed, since both influence the effective signal to noise ratio (SNR) their values should be carefully selected to obtain the best trade-off between observing asymmetry (increasing t_d) and higher EAP resolution (increasing G_{max}).

We have shown the theoretical EAP asymmetry sensitivity to a temperature-induced diffusivity gradient. Although we encourage further investigations on the subject, this work constitutes a fundamental step towards the design of a physical phantom for EAP asymmetry quantification through the DW signal.

References

1. Al-Shemmeri, T.: Engineering Fluid Mechanics. Ventus Publishing ApS., 17-18 (2012).
2. Callaghan, P.T.: Principles of nuclear magnetic resonance microscopy. Clarendon Press Oxford (1991).
3. Helenius, J., Soinne, L., Perkiö, J., Salonen, O., Kangasmäki, A., Kaste, M., Carano, R.A., Aronen, H.J., Tatlisumak, T.: Diffusion-weighted MR imaging in normal human brains in various age groups. American journal of neuroradiology 23, 194-199 (2002).
4. Holz, M., Heil, S.R., Sacco, A.: Temperature-dependent self-diffusion coefficients of water and six selected molecular liquids for calibration in accurate 1H NMR PFG measurements. Physical Chemistry Chemical Physics 2, 4740-4742 (2000).
5. Kozak, L., Bango, M., Szabo, M., Rudas, G., Vidnyanszky, Z., Nagy, Z.: Using diffusion MRI for measuring the temperature of cerebrospinal fluid within the lateral ventricles. Acta Paediatrica, 237-243 (2009).
6. Nicolas, R., Aubry, F., Pariente, J., Franceries, X., Chauveau, N., Saint-Aubert, L., Chollet, F., Breil, S., Celsis, P.: Water Diffusion in q-space Imaging as a Probe of Cell Local Viscosity

and Anomalous Diffusion in Grey and White Matter. The Open-Access Journal for the Basic Principles of Diffusion Theory, Experiment and Application, Diffusion-fundamentals.org 14, 3, 1-4 (2010).
7. Özarslan, E., Koay, C.G., Basser, P.J.: Remarks on q-space MR propagator in partially restricted, axially-symmetric, and isotropic environments. Magnetic Resonance Imaging 27, 834-844 (2009).
8. Pizzolato, M., Wassermann, D., Boutelier, T., Deriche, R.: Exploiting the Phase in Diffusion MRI for Microstructure Recovery: Towards Axonal Tortuosity via Asymmetric Diffusion Processes. Medical Image Computing and Computer Assisted Intervention, Munich, Germany (2015).
9. Tanner, J.E., Stejskal, E.: Restricted Self-Diffusion of Protons in Colloidal Systems by the Pulsed-Gradient, Spin-Echo Method. JCP 49(4), 1768-1777 (1968).